

A combined computational and functional approach identifies new residues involved in pH-dependent gating of ASIC1a

Luz Angélica Liechti, Simon Bernèche, Benoîte Bargeton, Justyna Iwaszkiewicz,
Sophie Roy, Olivier Michelin and Stephan Kellenberger

Supplemental Table and Figure file content

Suppl. Table S1	Analysis of the quality of homology models	2
Suppl. Table S2	pKa values and accessible surface area of Asp, Glu and His residues	3
Suppl. Table S3	Distance and relative orientation of pairs of Asp and Glu residues	6
Suppl. Figure S1	Alignment of ASICs and other family members	7
Suppl. Figure S2	Absence of window current in the E413Q/E418Q double mutant	9
Suppl. Table S4	pKa values calculated from the 3HGC-based model in the absence or presence of bound Cs ⁺ ions	10
Suppl. Table S5	Comparison of pH50-shifts relative to wt in this compared to previous studies	11
Suppl. Table S6	Numbering and species of ASIC residues cited in the discussion	12

Supplemental Table S1: Analysis of the quality of homology models

Model	C α RMSD with the template (Å) (sequence identity %)	Number of residues in favorable regions of the Ramachandran plot	Number of residues in the generously and additionally allowed regions of the Ramachandran plot	Number of residues in the disallowed regions of the Ramachandran plot
Model based on 2QTS template	0.5 (90%)	1048 (92.4%)	84 (7.5%)	2 (0.2%)
Model based on 3HGC template	0.4 (90%)	992 (91.1%)	95 (8.7%)	2 (0.2%)

The table indicates the parameters determined by PROCHECK (1) of the two homology models.

1. Laskowski, R. A., MacArthur, M. W., Moss, D. S., and Thornton, J. M. (1993) *J. Appl. Cryst.* **26**, 283-291

Supplemental Table S2. pKa values and accessible surface area of Asp, Glu and His residues

residue	position	pKa values			accessible surface area %
		unprotonated models		stepwise protonation	
		2QTS	3HGC	2QTS	
E63	1	18.35	19.97	-3.81	21
	2	19.77	18.22	p	
H70		1.86	4.50	-2.48	33
H72		4.08	0.17	3.85	20
H73		5.14	5.26	4.65	13
D78	1	2.11	9.98	-5.79	11
	2	8.42	2.61	p	
E79	1	10.69	12.36	p	1
	2	6.30	11.62	2.10	
E97	1	11.03	11.43	3.88	2
	2	10.94	11.54	p	
D107	1	3.65	5.09	2.81	0
	2	0.57	3.08	-0.45	
H110		4.62	4.56	4.63	10
E113	1	6.43	4.89	6.34	14
	2	6.17	2.72	6.07	
E123	1	3.76	4.51	3.76	31
	2	3.78	1.79	3.80	
D126	1	3.78	3.29	3.80	43
	2	3.79	4.23	3.80	
D131	1	4.01	3.47	4.00	34
	2	4.05	3.42	4.05	
E132	1	3.81	4.33	3.80	39
	2	3.79	4.35	3.80	
E136	1	5.39	4.69	5.53	33
	2	5.07	4.71	5.04	
D140	1	4.38	4.30	4.94	32
	2	5.17	4.25	4.51	
E156	1	4.44	6.18	4.18	23
	2	5.01	4.46	4.91	
D159	1	1.63	1.13	1.22	20
	2	3.70	2.70	3.50	
H163		2.95	-2.57	-0.15	0
D164	1	-0.82	-1.04	-1.49	10
	2	5.59	4.94	5.48	
D167	1	3.74	3.85	2.85	23
	2	3.71	3.70	2.87	
H173		4.93	5.63	4.52	20
E177	1	8.93	3.81	2.46	24
	2	10.59	3.56	p	
E182	1	4.34	3.61	4.13	44
	2	4.42	4.02	4.13	
D183	1	5.12	4.78	5.11	14
	2	3.00	4.78	4.75	

Supplemental Table S2, page 2

residue	position	pKa values			% surface area
		unprotonated models		stepwise protonation	
		2QTS	3HGC	2QTS	
D202	1	4.58	3.93	4.56	31
	2	4.25	3.93	4.78	
D212	1	6.18	4.72	3.93	0
	2	5.87	6.34	3.78	
E219	1	7.46	7.25	4.87	18
	2	9.43	8.32	4.90	
D223	1	6.91	5.65	5.46	0
	2	5.73	5.76	5.45	
D227	1	1.54	3.34	-0.85	33
	2	5.23	0.47	3.72	
E228	1	7.50	6.47	7.39	6
	2	5.25	4.17	5.13	
E235	1	5.30	3.54	5.20	29
	2	1.84	-1.01	1.86	
D237	1	8.50	6.07	2.26	21
	2	10.06	7.49	-1.20	
E238	1	12.95	6.23	1.14	2
	2	16.76	13.21	p	
E242	1	6.53	6.46	2.64	4
	2	8.35	6.81	p	
H250		4.49	2.30	3.34	2
D253	1	5.98	4.09	5.08	28
	2	5.11	4.08	5.03	
E254	1	5.95	2.86	5.83	4
	2	5.95	5.07	5.89	
D259	1	4.23	4.13	4.08	13
	2	4.27	3.27	4.13	
E277	1	6.97	9.61	3.05	1
	2	8.51	9.12	p	
D296	1	3.94	8.53	3.93	41
	2	3.94	6.28	3.94	
D298	1	4.54	8.33	3.49	42
	2	5.02	6.77	4.99	
D300	1	4.12	6.84	4.10	36
	2	4.18	10.18	4.20	
D303	1	4.14	6.90	3.94	32
	2	5.62	5.51	5.63	
D313	1	5.73	12.32	2.77	6
	2	5.04	16.96	4.60	
E315	1	12.13	9.09	p	1
	2	14.38	9.34	6.41	
E321	1	5.09	4.25	4.99	43
	2	5.15	4.25	5.05	
H329		0.33	0.84	-1.52	9

Supplemental Table S2, page 3

residue	position	pKa values			%
		unprotonated models		stepwise	
				protonation	surface area
2QTS	3HGC	2QTS			
D333	1	3.78	4.21	3.79	55
	2	3.79	4.26	3.79	
E340	1	4.87	3.55	4.60	25
	2	5.02	3.55	4.63	
E344	1	6.09	4.19	5.93	41
	2	4.78	4.19	5.49	
D347	1	12.00	8.90	6.35	2
	2	15.48	8.04	6.03	
D351	1	7.61	3.67	3.92	9
	2	10.64	7.27	p	
E355	1	6.46	5.20	5.88	14
	2	5.78	6.68	5.44	
D357	1	1.55	7.60	-0.11	0
	2	2.41	2.38	-1.14	
E359	1	4.30	4.36	4.28	42
	2	4.30	4.36	4.28	
E364	1	4.73	5.67	4.66	26
	2	4.73	5.47	4.69	
E375	1	5.87	7.53	4.53	7
	2	5.47	5.53	4.20	
E398	1	4.65	4.48	4.58	24
	2	3.36	1.33	3.31	
E403	1	3.96	-0.48	3.57	11
	2	1.79	4.37	1.52	
D409	1	10.45	10.08	1.15	0
	2	11.58	10.44	p	
E413	1	7.15	1.54	6.23	5
	2	7.05	5.10	6.40	
E418	1	8.76	10.80	6.97	5
	2	8.76	10.30	7.21	
E421	1	4.38	3.42	4.17	15
	2	3.49	4.30	3.25	
E427	1	4.16	7.38	3.90	26
	2	4.16	3.59	3.88	
D434	1	24.64	43.92	p	18
	2	15.44	36.43	-7.02	

pKa values were calculated as described in the text, for the two oxygen atoms of each Asp and Glu; His residues have 1 pKa value. Stepwise protonation, as described in the text; residues marked "p" were protonated in the model, and the pKa of the remaining residues was re-calculated. Iterations of protonation and re-calculation of pKa values of remaining, non-protonated side chains were done until all remaining side chains had a pKa < 5. For residues with pKa between 5 and 8, the pKa calculated in the round just before their own protonation is indicated.

Accessible surface area was calculated from the 2QTS-based model by using the COOR SEARCH function implemented in the CHARMM c34 molecular mechanics software. The relative accessible surface of acidic residues is shown as percentage of the surface of the isolated residue.

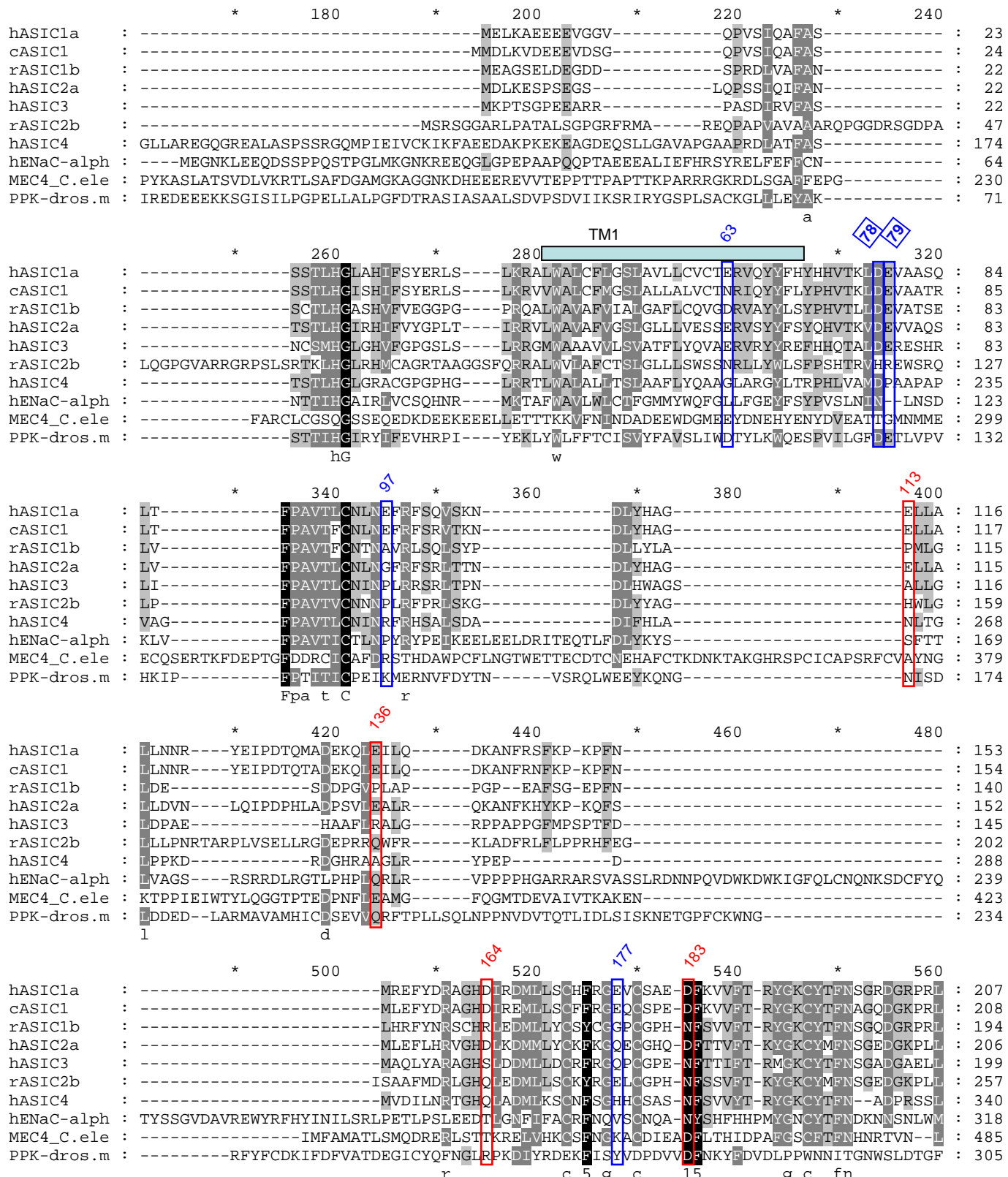
Supplemental Table S3

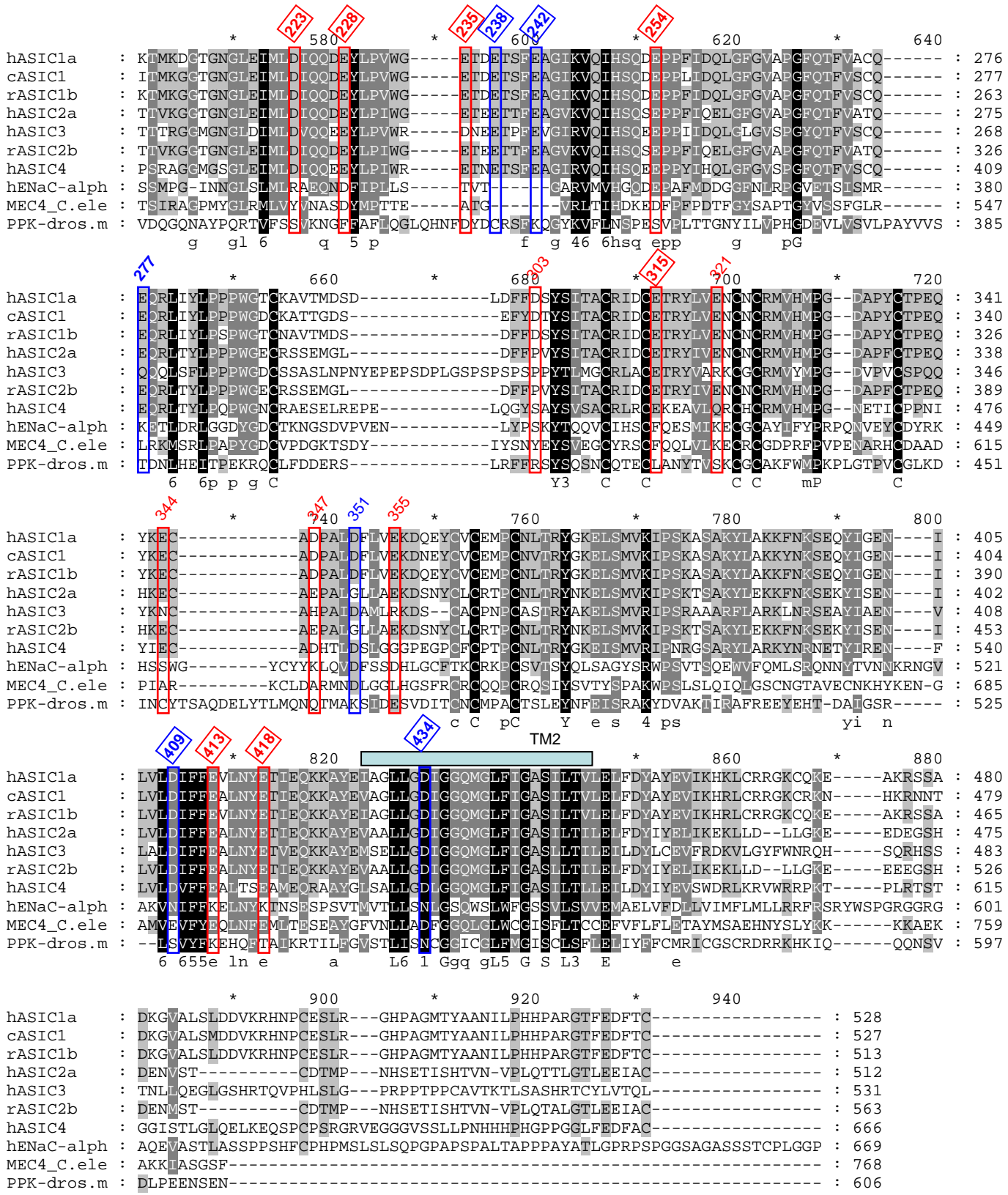
Distance and relative orientation of simple pairs of Asp and Glu residues

residue1	residue2	distance O-O* (Å)	relative orientation
E79	E418	5.56	towards each other
E97	E238	5.15	same orientation, 97 behind 238
E136	D140	4.03	~parallel
D164	D167	4.58	~parallel
E219	D409	2.95	on two anti-parallel beta-sheets, ~parallel
D227	E228	5.05	at ~70° Angle
E355	D351	3.73	parallel
D357	E359	6.85	similar orientation, 357 behind 359
E375	E413	4.96	towards each other, angle 120°

^{*}, distances were calculated in Chimera between the closest side-chain oxygen residues of the two acidic side chains from the human ASIC1a model based on the chicken ASIC1 structure 2QTS.

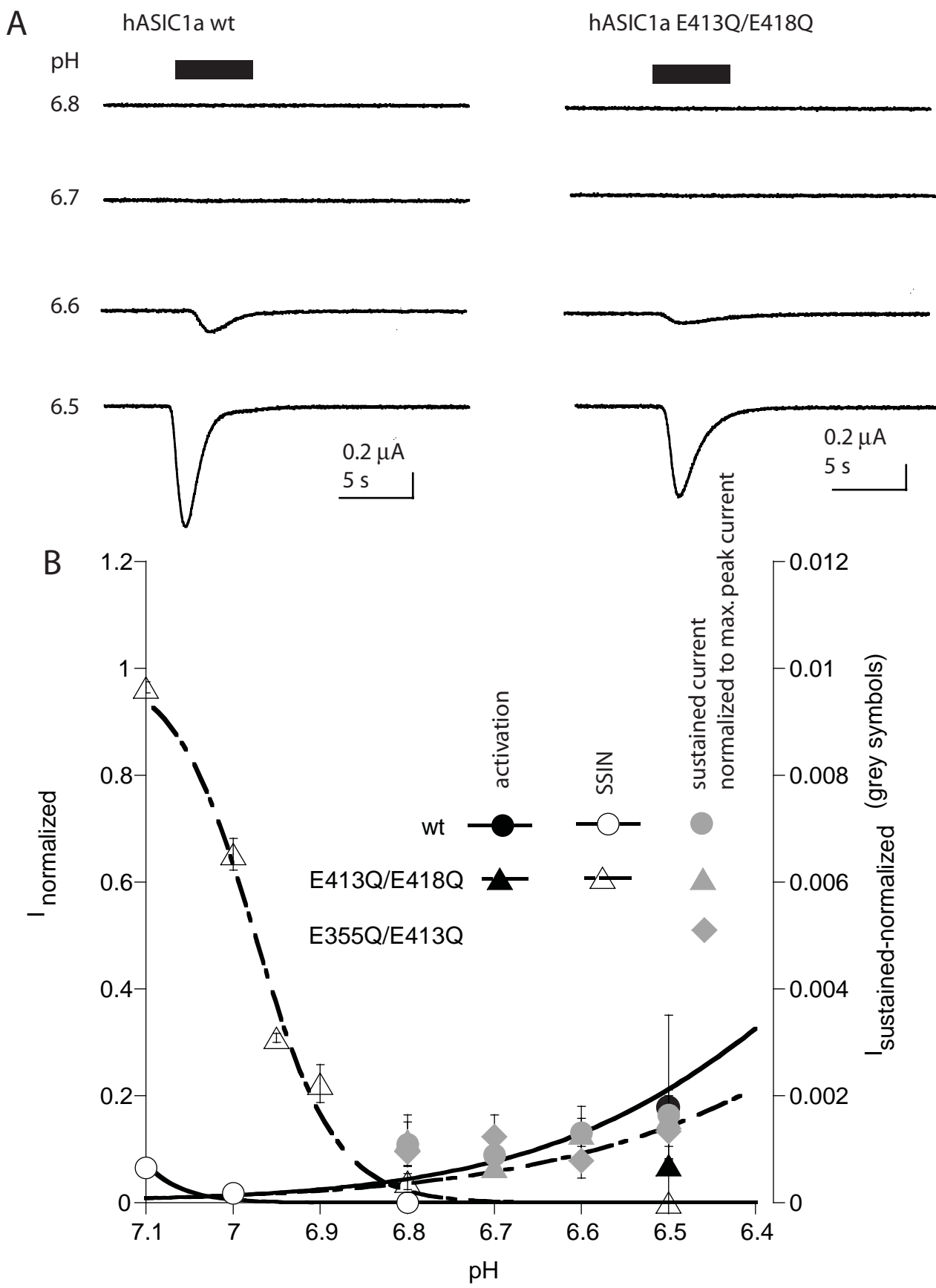
Supplemental Figure S1





Supplemental Figure S1. Alignment of ASICs and other family members. Alignment of ASIC1-4 and ENaC α (human), MEC-4 (C. elegans) and Pickpocket (PPK, drosophila), indicating Glu and Asp residues with pKa > 8 in blue, with 8 > pKa > 5 in red. Numbers of the amino acid residue in hASIC1a is indicated above the columns and is framed if the residue is conserved within the pH-gated ASIC subunits (ASIC1a, -1b, 2a and 3). GenBank accession numbers are AAB48981.1 (hASIC1a), AAY28986 (cASIC1), EDL86974 (rASIC1b), AAH75042 (hASIC2a), AAC64188 (hASIC3), EDM05432 (rASIC2b), EAW70762 (hASIC4), BAG65217 (ENaC- α), AAC47265 (MEC-4), and AAF53394 (PPK).

Supplemental Figure S2. Absence of window current in the E413Q/E418Q double mutant

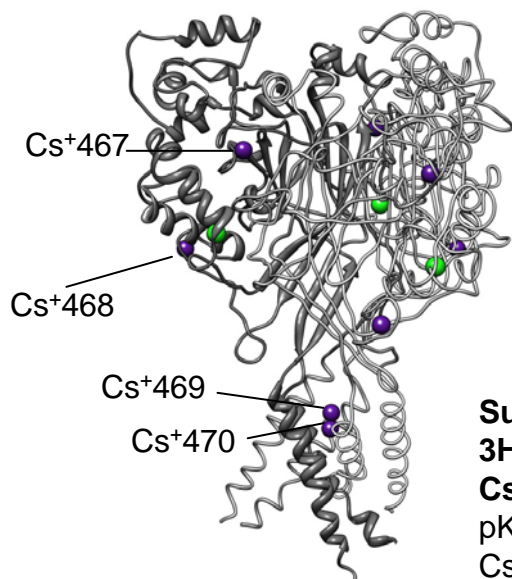


Supplemental Figure S2. Absence of window current in the E413Q/E418Q double mutant.

A, Typical traces in response to acidification to the pH indicated, during the time indicated by the black bar. B, Activation and SSIN curves of hASIC1a wt and the mutant E413Q/E418Q. For the pH range 7.1 to 6.4 (black lines, left axis). In grey, the sustained current amplitude, normalized to the peak current amplitude at pH 4.5, is indicated on a 100-fold expanded scale (right axis, n=5-8). This figure shows that in the two mutants represented, the currents inactivate as wt, and that there is no sustained current different from wt.

Supplemental Table S4. pKa values calculated from the 3HGC-based model in the absence or presence of bound Cs⁺ ions

proximity of Cs 467				proximity of Cs 468					
residue		3HGC	3HGC-Cs	delta	residue		3HGC	3HGC-Cs	delta
E97	1	11.43	11.42	-0.01	D296	1	8.53	8.53	0.00
	2	11.54	11.53	-0.01		2	6.28	6.29	0.01
E219	1	7.25	7.07	-0.18	D298	1	8.33	8.33	0.00
	2	8.32	8.01	-0.31		2	6.77	6.77	0.00
E235	1	3.54	3.54	0.00	D300	1	6.84	6.84	0.00
	2	-1.01	-1.01	0.00		2	10.18	10.18	0.00
D237	1	6.07	6.08	0.01	D303	1	6.90	6.90	0.00
	2	7.49	7.49	0.00		2	5.51	5.51	0.00
E242	1	6.46	6.40	-0.07	D313	1	12.32	12.32	0.00
	2	6.81	6.73	-0.08		2	16.96	16.97	0.01
D259	1	4.13	4.12	-0.01					
	2	3.27	3.27	0.00					
D347	1	8.90	8.90	0.00	proximity of Cs 469/470				
	2	8.04	8.04	0.00	residue		3HGC	3HGC-Cs	delta
D351	1	3.67	3.67	0.00	E427	1	7.38	4.46	-2.92
	2	7.27	7.27	0.00		2	3.59	1.42	-2.17
E355	1	5.20	5.20	0.00	D434	1	43.92	0.99	-42.93
	2	6.68	6.68	0.00		2	36.43	1.47	-34.96



Supplemental Table S4. pKa values calculated from the 3HGC-based model in the absence or presence of bound Cs⁺ ions.

pKa values were calculated for residues in the proximity of Cs⁺ ions in the 3IJ4 structure. The calculation was performed in the hASIC1a model derived from the 3HGC structure, in which the Cs⁺ ions had been placed. The table shows the pKa values for the 3HGC model, for the 3HGC model containing the Cs⁺ ions, and the column "delta" displays their difference. The inserted figure represents the 3IJ4 structure and indicates the position of Cs⁺ ions 467 and 468 of one subunit, and of Cs⁺ ions 469 and 470 (all shown in purple) in the channel pore. The Cl⁻ ions are shown in green.

Supplemental Table S5. Comparison of pH50-shifts relative to wt in this compared to previous studies

Residue	pH50-shift relative to wt in this study	compared mutation	pH50-shift relative to wt	Reference
E113	< 0.1	ASIC2a E112Q	< 0.1	(1)
E136	< 0.1	ASIC2a E135Q	-0.13	(1)
D164	-0.10	ASIC2a D163N	< 0.1	(1)
D183	-0.10	ASIC2a D182N	+0.34	(1)
D223	< 0.1	rASIC1a D223N	< 0.1	(2)
E228	-0.13	rASIC1a E228Q	< 0.1	(2)
E235	< 0.1 ^b	rASIC1a E235Q	-0.2	(2)
E254	< 0.1	rASIC1a E254Q	< 0.1	(2)
E344	< 0.1	rASIC1a E342Q	< 0.1	(2)
D347	-0.19 ^a	cASIC1 D346N	-0.3 ^c	(3)
E413Q	-0.10	rASIC1a E411Q	-0.1	(2)
E418Q	-0.19 ^a	rASIC1a E418Q	-0.15	(2)

The pH50 values of mutants of D303, E315, E321 and E355 have not been determined previously, and SSIN has been analyzed for none of these residues to our knowledge. pH50 data are reported from ASIC1 where available, and for some mutants from ASIC2a. rASIC1a, rat ASIC1a ; cASIC1, chicken ASIC1. ^a, difference from wt statistically tested ($p < 0.05$). ^b, nH, Hill coefficient significantly different from wt ($p < 0.05$). ^c, for this mutant a marked decrease in the Hill coefficient was reported.

Supplemental Table S6. Numbering and species of ASIC residues cited in the discussion

Residue in this study	Cited study		
	Position	Species ^a	Reference
Y71	72	r	(4)
H72	72	r	(2)
H73	73	r	(2)
H73	72	ASIC2a	(5)
D78	78	r	(2)
E79	79	rASIC3	(6)
K105	105	r	(2)
N106	106	r	(2)
D107	107	r	(2)
R190	190	r	(2)
E235	235	r	(2)
D237	237	r	(2)
E238	238	r	(2)
D253	253	r	(2)
E254	254	r	(2)
W287	288	r	(4)
D347	346	c	(3)
D351	350	c	(3)
D357	357	h	(7)
D357	355	r	(2)
Q358	358	r	(8)
Q358	358	h	(7)
E359	359	r	(8)
E413	411	r	(2)
E418	416	r	(2)

^a, and indication of ASIC isoform, if different from ASIC1a. r, rat; c, chicken, h, human.

References for Tables S5 and S6

- Smith, E. S., Zhang, X., Cadiou, H., and McNaughton, P. A. (2007) *Neurosci Lett* **426**, 12-17
- Paukert, M., Chen, X., Polleichtner, G., Schindelin, H., and Grunder, S. (2008) *J Biol Chem* **283**, 572-581
- Jasti, J., Furukawa, H., Gonzales, E. B., and Gouaux, E. (2007) *Nature* **449**, 316-323
- Li, T., Yang, Y., and Canessa, C. M. (2009) *J Biol Chem* **284**, 4689-4694
- Baron, A., Schaefer, L., Lingueglia, E., Champigny, G., and Lazdunski, M. (2001) *J. Biol. Chem.* **276**, 35361-35367
- Cushman, K. A., Marsh-Haffner, J., Adelman, J. P., and McCleskey, E. W. (2007) *J Gen Physiol* **129**, 345-350
- Sherwood, T., Franke, R., Conneely, S., Joyner, J., Arumugan, P., and Askwith, C. (2009) *J Biol Chem* **284**, 27899-27907
- Coric, T., Zheng, D., Gerstein, M., and Canessa, C. M. (2005) *J Physiol (Lond)* **568.3**, 725-735